

Research Article

Liposome-coated metal-organic frameworks as the efficient drug delivery system for therapeutic applications

Natchanon Ratanapun^a, Komgrit Eawsakul^b, Naruemon Setthaya^c, Chakkresit Chindawong^c, Wei Guo Song^d, Chawan Manaspon^{a,e,*}, Pagasukon Mekrattanachai^{c,f,*}

^a Biomedical Engineering Institute, Chiang Mai University, Chiang Mai 50200, Thailand

^b Department of Applied Thai Traditional Medicine, School of Medicine, Walailak University, Nakhon Si Thammarat 80160, Thailand

^c School of Chemistry, Faculty of Science, University of Phayao, Phayao 56000, Thailand

^d Beijing National Laboratory for Molecular Sciences, Laboratory of Molecular Nanostructures and Nanotechnology, CAS Research/Education Center for Excellence in Molecular Sciences, Institute of Chemistry, Chinese Academy of Sciences, Beijing 100190, China

^e Biomedical Engineering and Innovation Research Center, Chiang Mai University, Chiang Mai 50200, Thailand

^f Unit of Excellence on Advanced Nanomaterials, University of Phayao, Phayao 56000, Thailand

ARTICLE INFO

Keywords:

Liposome
 Metal-organic frameworks (MOFs)
 Cellular uptake
 Drug delivery system (DDS)
 Fluorescent dyes

ABSTRACT

Zeolitic imidazole framework-8 (ZIF-8) particles, composed of zinc ions (Zn^{2+}) and 2-methylimidazolate, were used as carriers for incorporating iron oxide (Fe_3O_4) nanoparticles, resulting in $Fe_3O_4@ZIF-8$ particles. Due to the toxicity of Zn^{2+} to cell membranes, liposomes were employed to reduce this toxicity. Fluorescent dyes were loaded into ZIF-8 or $Fe_3O_4@ZIF-8$ nanoparticles as the mock drugs to facilitate tracking during cellular studies. The encapsulation efficiency of fluorescein (Flu) and Nile red (NiR) in the MOFs was calculated to be around 40%–60%. A burst release of Flu was observed under acidic conditions within 30 min, while natural PBS was significantly released in 6 h. The release kinetic of the whole platform was fitted with the Higuchi equation which referred to diffusion release. Liposome coating significantly decreased the toxicity of the MOFs, as evidenced by an increase in IC_{50} values from approximately 30 to 120 $\mu g/mL$. The LDH release from L929 cells was confirmed when particles were used at exceeding 100 $\mu g/mL$. The cellular uptake of the liposome-coated dye-loaded MOFs was confirmed after 3-hour incubation. These findings suggested that liposome-coated MOFs could be served as an alternative carrier in biomedical engineering field.

1. Introduction

Drug delivery system (DDS) is a technology which designed to transport drugs within the body. It typically consists of three main components: a carrier, drugs, and targeting ligands [1]. Using targeting ligands, the system is usually designed to deliver drugs to specific locations in the body, which can improve treatment effectiveness and minimize side effect on healthy tissues. Several drug carriers used in the market are nanoparticles, liposomes, micelles, dendrimers, iron oxide, and metal-organic frameworks (MOFs) [2–5]. In recent years, nanoparticles have shown great potential in DDS because the encapsulation of drugs in nanoparticles can improve the therapeutic index and reduce the adverse side effects [6].

MOFs are porous materials synthesized from metal ions and organic ligands which can be connected to each other via coordination into three-dimensional frameworks, resulting highly ordered structure. MOFs are particularly attractive as drug carriers due to their high sur-

face area and porosity offering potential for drug loading [5,7,8]. Numerous types of MOFs have existed globally, including MOF-5 [9], MIL-53, MOF-808 [10], ZIF-7, and ZIF-8 [7,8,11,12]. Zeolitic imidazole framework-8 (ZIF-8), a specific type of MOF constructed from Zn^{2+} and 2-methylimidazole linkers, is particularly notable for its stability and high surface area, facilitating effective drug loading and controlled release. These characteristics make ZIF-8 a promising material for enhancing the delivery and therapeutic efficacy of drugs, particularly in targeted and sustained release applications [13]. ZIF-8 was applied as drug carriers in several works, for example, pH-responsive resveratrol-loaded ZIF-8 nanoparticles modified with tannic acid (TA) was developed as pH-responsive material to enhance biocompatibility and controlled-release of resveratrol for the treatment of colon cancer [14]. The resulting demonstrated significant potential in promoting apoptosis (programmed cell death) in colon cancer cells, suggesting an effective strategy for targeted cancer therapy [14]. Another work showed that ZIF-8 was applied to enhance the electrochemical signal

* Corresponding authors.

E-mail addresses: chawan.m@cmu.ac.th (C. Manaspon), pagasukon.me@up.ac.th (P. Mekrattanachai).

<https://doi.org/10.1016/j.chphma.2025.08.004>

Received 7 February 2025; Received in revised form 27 August 2025; Accepted 31 August 2025

Available online 10 September 2025

2772-5715/© 2025 The Authors. Publishing Services by Elsevier B.V. on behalf of KeAi Communications Co. Ltd. This is an open access article under the CC BY-NC-ND license (<http://creativecommons.org/licenses/by-nc-nd/4.0/>)

of the sensor for detecting mitoxantrone [15]. In 2017, Kaur et al. synthesized 6-mercaptopurine (6-MP), the anti-leukemia drug, loaded in situ into the ZIF-8 nanoparticles for drug delivery application. The 6-MP was successfully loaded into ZIF-8 resulting in the formation of 6-MP@ZIF-8. Further, the 6-MP@ZIF-8 exhibited much faster release of drug in acidic environment as compared with release in pH 7.4 because of the decomposition of ZIF-8 structure. This indicated the potential of ZIF-8 to be used as a carrier for controlled delivery of 6-MP against cancer cells [8]. In 2020, Ma et al. synthesized paclitaxel (PTX) loaded on cystamine modified ZIF-8 for gastric cancer treatment. The drug release of this prepared material was studied under different pH and glutathione (GSH) concentrations. Higher glutathione concentration and acidic pH were favorable to the release of PTX. Moreover, the release of PTX from cystamine modified ZIF-8 provided a higher tumor-killing effect than free paclitaxel solution [12]. However, it has been reported that ZIF-8 can generate high concentration of Zn^{2+} , leading to the production of reactive oxygen species (ROS) in the cytoplasm. ROS can inhibit the glutathione reductase (GR) enzyme, which reduces the production glutathione in cells. Consequently, the inflammation response in the cell would increase, leading to the upregulation of inflammation-related genes such as *CCL4* and *IL6*. Ultimately, this could result in cell necrosis [16].

Superparamagnetic iron oxide nanoparticles (Fe_3O_4) are a class of versatile materials with significant potential in the biomedical field, particularly for diagnostics and therapeutics [19,20]. They are commonly employed as contrast agents in magnetic resonance imaging (MRI) for cancer detection, as well as drug carriers for targeted delivery to specific organs and magnetic hyperthermia agents for tumor ablation [20,21]. However, the use of bare Fe_3O_4 nanoparticles is limited by several drawbacks. Their inherent bulk structure restricts drug conjugation to the surface, leading to low encapsulation efficiency, and excessive concentrations can induce the formation of free radicals, raising toxicity concerns [22]. To overcome these limitations, an engineering of a core-shell composite has been studied by encapsulating Fe_3O_4 nanoparticles within a ZIF-8 frameworks. This novel Fe_3O_4 @ZIF-8 system combined the superparamagnetic properties of the core with the structural integrity of the shell [17,18]. While both ZIF-8 and Fe_3O_4 @ZIF-8 possessed desirable physical properties for biomedical use, key challenges such as their potential cytotoxicity, uncontrolled drug release in acidic environments, and limited cellular uptake must be thoroughly investigated to advance their application as a reliable drug delivery platform. Though ZIF-8 offered several advantages of drug delivery application, its potential cytotoxic effects remain a concern. Moreover, ZIF-8 has been reported a cytotoxic effect on L929 fibroblast cells, with an IC_{50} value of approximately 30 $\mu\text{g}/\text{mL}$ [17,18]. Hence, to enhance biocompatibility, ZIF-8 should be modified with supplementary materials such as polymers or lipid bilayers.

Liposomes are nontoxic small vesicles with spherical in shape that can be produced from cholesterol, non-toxic surfactants, sphingolipids, glycolipids and long chain fatty acids. Liposomes are also applied as drug carriers because they can be loaded with a variety of molecules such as small drug molecules, proteins, nucleotides and even plasmids [23,24]. For drug delivery application, liposome was chosen to reduce the toxicity effect on the cell. According to the suitable properties of ZIF-8 and liposome for DDS, both materials were investigated as drug carriers. However, a few studies have been done using liposome-coated ZIF-8/ Fe_3O_4 @ZIF-8 for DDS.

Therefore, in this work, liposome-coated ZIF-8 or core-shell Fe_3O_4 @ZIF-8 were synthesized by facile method for drug delivery application. ZIF-8 and Fe_3O_4 @ZIF-8 nanomaterials were employed as drug carriers with magnetic property derived from Fe_3O_4 particles. Liposome was used to coat on these nanomaterials to enhance the biocompatibility and cellular uptake. Moreover, fluorescent dyes (nile red; NiR and fluorescein; Flu) were used as the mock drugs for studying the mechanism of drug release. Both dyes were loaded independently into both MOFs (ZIF-8 and Fe_3O_4 @ZIF-8). The suitable concentration of these dyes was

evaluated using the encapsulation efficiency (%EE) value. After that, the optimized dyes-loaded MOFs were coated with liposomes, and bare liposome was also fabricated as control. Next, the prepared samples were characterized through various methods including, size measurement, polydispersity index (PDI), and zeta potential. Furthermore, the morphology of the prepared materials was studied from both TEM and SEM techniques. Additionally, the prepared samples were applied for drug release study, in vitro cytotoxicity test by MTT and LDH methods using L929 cells and cellular uptakes study. Thus, the novelty of this work mentioned the synergistic combination of a MOFs core (ZIF-8 or Fe_3O_4 @ZIF-8) with a liposome coating. This design created a multifunctional platform that addresses the limitations of toxicity, burst release, and cellular uptake in a single system, representing a significant advancement over existing drug delivery platforms.

2. Materials and methods

2.1. Chemical and reagents

Cholesterol (CHOL) and fluorescein sodium salt (Flu) were purchased from Sigma-Aldrich (USA). Nile red (NiR) was purchased from Tokyo Chemical Industry (TCI) CO., LTD (Japan). 1,2-dipalmitoyl-sn-glycero-3-phosphocholine (DPPC) was purchased from Avanti Polar Lipid, Inc (USA). Zeolitic imidazolate framework-8 (ZIF-8) and core shell iron oxide nanoparticle-loaded zeolitic imidazolate framework-8 (Fe_3O_4 @ZIF-8) were prepared as described in our previous work [17,18]. The L929: NCTC clone 929 cell line (IFO50409) was purchased from the Japanese Collection of Research Bioresources Cell Bank (JCRB, Japan). Dulbecco's modified Eagle medium (DMEM), fetal bovine serum (FBS), and antibiotic solution were purchased from Gibco: Thermo Fisher Scientific (USA). Triton X-100, phosphate buffer saline tablets (PBS), dimethyl sulfoxide (DMSO), and MTT reagent ((3-(4,5)-dimethylthiazol-2-yl)-2,5-diphenyl tetrazolium bromide) were purchased from Amresco Inc. (USA). LDH cytotoxicity assay kit (88954) was purchased from Pierce® Thermo scientific (USA).

2.2. Liposome fabrication

Initially, DPPC:CHOL (lipid phase) ratios of 2:1, 3:1, and 4:1 (w/w) were used to optimize liposome production [25]. A mixture of DPPC and CHOL was dissolved in ethanol at 0.25 mg/mL and heated to 60 °C until a clear solution formed. This lipid phase was then injected dropwise into an aqueous phase (Milli-Q water) at a 1:4 ratio (v/v) of lipid phase : aqueous phase, and the mixture was stirred at 60 °C to completely remove ethanol. Finally, the liposome suspension was sonicated for 5 min and stored at room temperature. To prepare liposome-coated ZIF-8 or Fe_3O_4 @ZIF-8 materials, the respective MOF was added to the lipid phase (1 mg/mL) before injection into the aqueous phase.

2.3. Preparation of liposome-coated dye-loaded-MOFs

MOFs (both ZIF-8 and Fe_3O_4 @ZIF-8) were used as drug vehicles to encapsulate the mock drugs (Flu and NiR). Hydrophilic Flu was prepared in Milli-Q water, while hydrophobic NiR was prepared in ethanol, both at concentrations ranging from 0.1 to 5 $\mu\text{g}/\text{mL}$. Either ZIF-8 or Fe_3O_4 @ZIF-8 was added to the dye solution and the mixture was shaken for 24 h. The samples were then centrifuged at 15000 rpm for 10 min, and the supernatant was collected to analyze the unloaded dyes. The solid residues were washed with water, dried at 60 °C for 3 h, then coated with liposome using the previously described method. The amount of unload Flu and NiR were quantified using a microplate reader spectrophotometer (TECAN Infinite M Plex, Switzerland) at excitation/emission wavelengths of 460/518 nm for Flu and 588/625 nm for NiR. Encapsulation efficiency (%EE) was calculated using Eq. (1).

$$\%EE = \frac{\text{mass of initial dye} - \text{unloaded dye}}{\text{mass of initial dye}} \times 100. \quad (1)$$

2.4. *In vitro* dyes release study and release kinetic

MOFs with different concentrations (1, 5, and 10 mg/mL) in PBS (pH 4 or 7.4) were incubated at 37 °C. At predetermined time points (30 min, 1, 2, 6, and 24 h), the solution was refreshed, and the amount of dye released was measured. For liposome-coated MOFs, samples were placed in a dialysis bag and immersed in PBS (pH 4 or 7.4). The solution was collected at different time points and the amount of dye released was measured using fluorescence intensity. To understand the release mechanism of uncoated and liposome-coated dye-loaded MOFs, the cumulative release data was fitted with the following mathematics equation (Eqs. (2)–(5)) [26,27]. Where Q_t is the cumulative amount of drug, Q_0 is the initial amount of drug, t is time. The constant, k , represents a fixed value within an equation. Specific types of constants include k_0 for zero-order equations, k_1 for first-order equations, k_H for Higuchi's equation, and k_{HC} for the Hixson-Crowell equation.

$$\text{Zero order : } Q_t = Q_0 + k_0 t, \quad (2)$$

$$\text{First order : } Q_t = Q_0 e^{-k_1 t}, \quad (3)$$

$$\text{Higuchi : } Q_t = k_H \sqrt{t}, \quad (4)$$

$$\text{Hixson - Crowell : } \sqrt[3]{Q_0} - \sqrt[3]{Q_t} = k_{HC} t. \quad (5)$$

2.5. Characterization of liposome-coated/uncoated dyes-loaded MOFs

The morphology of samples was examined using a mini-scanning electron microscope (mini-SEM) (JEOL JCM-7000 NeoScope™) and transmission electron microscope (TEM) (JEOL JEM-2100). A drop of the sample was placed onto a copper grid for 2 min, followed by blotting. The samples were then negatively stained with 3% phosphotungstic acid (TED PELLA, Inc.) for 1 min. Lastly, the copper grid was dried overnight. In addition, size, polydispersity Index (PDI), and zeta potential were measured using dynamic light scattering (DLS) (Malvern Instruments, UK) at 25 °C with a detection angle of 173°. For DLS, all samples were prepared at a concentration of at least 1 mg/mL of liposome in a Milli-Q water. Before measurement, each sample was sonicated for 5 min to avoid any aggregates.

2.6. Cytotoxicity study

L929 cells (10000 cells/well) were seeded in a 96-well plate and incubated at 37 °C, 5% of CO₂ to allow cell adhesion and growth. The cells were treated with 100 µL of various concentrations of each sample (uncoated MOFs and liposomes-coated MOFs). It should be noted that all samples must be prepared in serum-free medium. After 24 h incubation, MTT reagent (0.5 mg/mL) was then added into each well and incubated for 1 h. The formazan product was dissolved by DMSO before measuring the absorbance at 570 nm via microplate reader (TECAN Infinite M plex, Switzerland). The activity of cytoplasmic enzymes produced by injured cells was measured by the adapted instructions of Pierce LDH Cytotoxicity assay kit. The supernatant of treated medium after 24-hour incubation were collected and mixed with substrate solution. The reaction was incubated for 30 min. Cell lysis buffer was used and treated as a positive group. Finally, the samples were measured the absorbance at 490 nm within 1 h after adding the stop solution.

2.7. Cellular uptake

In brief, the L929 cells were seeded into a 12-well plate at 10000 cells per well. Then, 2 mL of sample suspensions (50 µg/mL of liposome-coated dye-loaded MOFs) were placed into each well and incubated for 3, 6, and 24 h using phenol red-free culture medium. The suspension

was removed and the cells were washed with PBS. The cells were then maintained in PBS and observed for qualitative study under a fluorescent microscope (EVOS M5000 microscope, Invitrogen™).

2.8. Statistical analysis

All results were performed in at least triplicate and the results were expressed as mean and standard deviation (SD). For comparisons between two group, statistical analysis was performed using a *t*-test. All statistical analysis and graphical illustrations were performed using Prism 8 (GraphPad Software, CA, USA) in which an acceptance *p*-value less than 0.05.

3. Results and discussion

3.1. Characterization of ZIF-8 and Fe₃O₄@ZIF-8 nanomaterials

ZIF-8 and Fe₃O₄@ZIF-8 were synthesized using the precipitation method described in our previous work. Fe₃O₄ nanoparticles were also incorporated into the ZIF-8 structure as potential MRI contrast agents [17,18]. The XRD results confirmed ZIF-8 and Fe₃O₄@ZIF-8 crystalline structure, Fig. 1(a). The crystalline structure of the synthesized materials was characterized by X-ray diffraction (XRD) analysis, and the results are presented in Fig. 1(a). The XRD pattern of the synthesized ZIF-8 (red line) showed sharp and distinct diffraction peaks at 2θ values of approximately 7.3°, 10.3°, 12.6°, 14.7°, 16.5°, and 18.0°, which were in excellent agreement with the peaks of the simulated ZIF-8 pattern (green line), Fig. 1(a). The XRD pattern of the Fe₃O₄ nanoparticles (black line) mentioned broad diffraction peaks at 2θ values of approximately 30.1°, 35.5°, 43.1°, 53.4°, 57.0°, and 62.6°. The XRD pattern of the Fe₃O₄@ZIF-8 composite (blue line) showed the characteristic diffraction peaks of ZIF-8, indicating that the ZIF-8 crystal structure was maintained after encapsulation of the Fe₃O₄ nanoparticles. The presence of a small peak at approximately 35.5° (marked with an asterisk) confirmed the successful incorporation of Fe₃O₄ nanoparticles within the ZIF-8 frameworks [17,18]. The TEM analysis revealed spherical Fe₃O₄ nanoparticles with a size of ~246 nm (Fig. 1(c)), whereas the size of cubic ZIF-8 was around ~240 nm (Fig. 1(b)). Thus, the Fe₃O₄@ZIF-8 core-shell structures had a size of 192–477 (~340) nm. Studies suggested that ZIF-8 nanoparticles may damage cell membranes, causing the production of harmful molecules inside cells (reactive oxygen species: ROSS) and ultimately leading to cell death. Therefore, using pure ZIF-8 exceeding 35–50 µg/mL was not advised for further *in vitro* research [17,18]. Moreover, it has been reported that the median lethal dose (LD50) of ZIF-8 is 350 µg/mL for zinc ions and 1.13 g/kg for the organic ligand (2-MeIm) [16]. To minimize the potential toxicity of ZIF-8 nanoparticles, it may be coated with liposomes and loaded by fluorescent dyes as mock drugs for tracking *in vitro* experiments.

3.2. Characterization of liposome-coated/uncoated dyes-loaded MOFs

The solvent injection method was chosen for liposome preparation due to its simplicity of scaling up for future production compared to others. In this study, different ratios of DPPC:CHOL (2:1, 3:1, and 4:1) were employed. Liposome prepared with the ratio at 2:1 was selected for further study due to its smaller particle size (166.4 ± 36.5 nm) which was suitable for drug carrier property [28]. In contrast, liposome sizes increased with increasing lipid phase ratio. CHOL was incorporated into the liposome layer to enhance their stability and minimize aggregation by increasing membrane rigidity [29]. As the measured sizes were 166.4 ± 36.5, 252.2 ± 53.1, and 283.8 ± 16.5 nm for DPPC:CHOL ratios of 2:1, 3:1, and 4:1, respectively. The 2:1 ratio exhibited a zeta potential of -21.3 ± 5.6 mV and the PDI value of 0.10 ± 0.07, Table 1.

An initial assessment of liposome size was performed using the Tyndall effect, which detected light scattering by colloidal particle [30]. As expected, the liposome suspensions exhibited the Tyndall effect

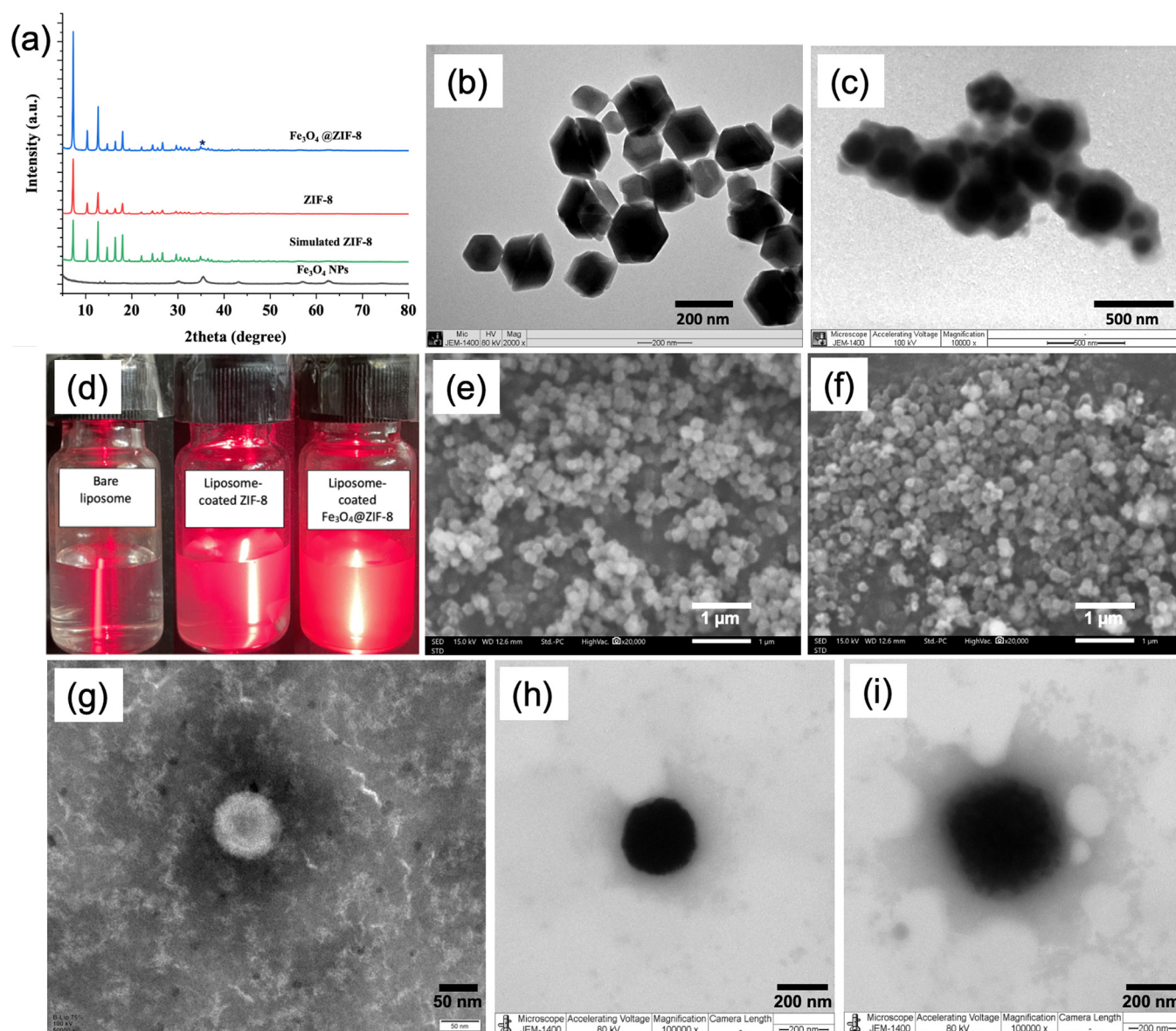


Fig. 1. The characterization of MOFs, liposome-coated MOFs, and MOFs. (a) X-ray diffraction (XRD) of Fe_3O_4 nanoparticles (NPs), ZIF-8, simulated ZIF-8 and Fe_3O_4 @ZIF-8. (b) TEM image of ZIF-8, scale bar = 200 nm. (c) TEM image of Fe_3O_4 @ZIF-8, scale bar = 500 nm. (d) Tyndall's effect of liposome group. (e) SEM image of ZIF-8, scale bar = 1 μm . (f) SEM image of Fe_3O_4 @ZIF-8, scale bar = 1 μm . (g) TEM image of bare liposome, scale bar = 50 nm. (h) TEM image of liposome-coated ZIF-8, scale bar = 200 nm. And (i) TEM image of liposome-coated Fe_3O_4 @ZIF-8, scale bar = 200 nm.

Table 1

Hydrodynamic size, polydispersity index (PDI), and zeta potential of nanoparticle samples (Mean \pm SD) by DLS.

Condition	Size (nm)	Polydispersity Index (PDI)	Zeta Potential (mV)
Bare Liposome	166.4 \pm 36.5	0.10 \pm 0.07	-21.3 \pm 5.6
liposome-coated ZIF-8	331.1 \pm 58.8	0.57 \pm 0.05	-23.2 \pm 1.5
liposome-coated Fe_3O_4 @ZIF-8	228.1 \pm 46.4	0.43 \pm 0.11	-22.6 \pm 4.2
liposome-coated Flu-loaded ZIF-8	215.53 \pm 25.76	0.12 \pm 0.01	-12.25 \pm 2.07
liposome-coated Flu-loaded Fe_3O_4 @ZIF-8	169.13 \pm 42.83	0.46 \pm 0.05	-14.27 \pm 1.62
liposome-coated NiR-loaded ZIF-8	247.57 \pm 45.08	0.37 \pm 0.03	-13.30 \pm 0.78
liposome-coated NiR-loaded Fe_3O_4 @ZIF-8	183.17 \pm 14.93	0.39 \pm 0.02	-16.67 \pm 0.47

(Fig. 1(d)), indicating a size sufficient for light scattering. The morphology of overall surface of ZIF-8 and Fe_3O_4 @ZIF-8 were studied by SEM technique. ZIF-8 and Fe_3O_4 @ZIF-8 under SEM images are presented in Fig. 1(e) and (f), respectively which were consistent with previous studies [17,18]. Herein, ZIF-8 and Fe_3O_4 @ZIF-8 had average particle sizes of ~ 159.6 and ~ 204.0 nm and zeta potentials of ~ 16.6 and ~ 10.6 mV

as determined by DLS using ethanol as a solvent. A high-resolution TEM image in Fig. 1(g) illustrates the structure and details of bare liposome, a negative staining was used to enhance visualization of the lipid bilayer boundaries. The observed structure of the bare liposome was around 100 nm (the size from DLS was ~ 166.4 nm). Fig. 1(h) shows liposome-coated ZIF-8, with the surrounding light gray color representing the li-

posome layer. DLS analysis revealed a size of liposome-coated ZIF-8 approximately 331.1 ± 58.8 nm (PDI 0.57 ± 0.05) and a zeta potential of -23.2 ± 1.5 mV. After coating this liposome on the Fe_3O_4 @ZIF-8 (Fig. 1(i)), a multilayer liposomal structure was also observed with the average size around 228.1 ± 46.4 nm (PDI 0.43 ± 0.11), and the zeta potential was -22.6 ± 4.2 mV, Table 1.

For liposome-coated dye-loaded MOFs materials, the particle sizes of liposome-coated Flu-loaded ZIF-8 and Fe_3O_4 @ZIF-8 were approximately 215.5 and 170.0 nm, respectively, with PDIs of 0.12 and 0.46. Their zeta potentials were -12.3 and -14.3 mV. For NiR-loaded MOFs, liposome coating increased particle sizes to approximately 247.6 and 183.2 nm for liposome-coated NiR-loaded ZIF-8 and NiR-loaded Fe_3O_4 @ZIF-8, respectively (PDIs of 0.37 and 0.39) and resulted in zeta potentials of -13.3 and -15.7 mV, Table 1.

3.3. Encapsulation efficiency (%EE) study of dye-loaded MOFs

In order to determine the best %EE while comparing with different dye concentrations, two distinct fluorescent dyes with opposing properties were used: NiR, which is hydrophobic, and Flu, which is hydrophilic. Fig. 2(a) shows the %EE of Flu-loaded MOFs, the highest %EE of both samples was observed at 1 $\mu\text{g}/\text{mL}$ of Flu concentration. Interestingly, increasing the initial Flu concentration from 1 to 2 $\mu\text{g}/\text{mL}$ did not significantly improve %EE value in both of ZIF-8 and Fe_3O_4 @ZIF-8, which might be due to limited loading capacity. However, Fe_3O_4 @ZIF-8 achieved a higher %EE value ($>70\%$) for Flu compared to ZIF-8. The encapsulation process for NiR differed from using Flu which is shown in Fig. 2(b). The %EE value was decreased when the NiR concentration was increased which might be due to the low coordination between dye and nanomaterials' surface. Although, ZIF-8/ Fe_3O_4 @ZIF-8, with their large surface area, provided numerous sites for physical adsorption of NiR molecules, they might adsorb only on the MOFs's surface with weak interaction, so they easily removed into dye solution. Thus, the 1 $\mu\text{g}/\text{mL}$ of dye was chosen as the optimal concentration in subsequent studies. Therefore, the different solubility of the dyes and chemical structure resulted in different %EE values due to different interaction and the location in MOFs structure [31]. For comparison, previous studies reported doxorubicin-encapsulated ZIF-8 exhibiting improved thermal stability using PXRD analysis and ZIF-8 loaded physcion (PHY) which had the encapsulation efficiency of $\sim 88\%$ by using a nano-precipitation technique, highlighting the high encapsulation capacity of ZIF-8 [32,33].

3.4. In vitro dyes release study and release kinetic

The release study of encapsulated dyes was investigated under two conditions consisting of acidic (pH 4.0) and physiological (pH 7.4) environment in PBS solution. Unfortunately, NiR did not dissolve in PBS, limiting the release study. MOFs are known to be pH sensitive because acidic environments can trigger the breakdown of the MOF structure due to reactions between hydronium ions and the metal ligand bonds [34]. For uncoated MOFs, released dyes were collected from the supernatant after centrifugation, whereas liposome-coated MOFs were collected from the external aqueous phase of the dialysis bag.

Fig. 2(c) shows the release profile of Flu-loaded ZIF-8 in acidic PBS with completed release occurring within 2 h. for all initial mass (1–10 mg). In contrast, only 1 mg of Flu-loaded ZIF-8 completely released of Flu after 6 h. at physiological pH (Fig. 2(d)). Similar trends were observed for Flu release from Fe_3O_4 @ZIF-8 nanoparticles, Fig. 2(e). The acidic condition raised the complete release within 2 h, while slow release was observed at pH 7.4. The higher mass affected the lower release as its property of the carrier and dyes. In Figs. 2 (d)(f), higher mass of the nanoparticles (10 mg) exhibited slower release, reaching only around 50% and 25% release at 24 h for Fe_3O_4 @ZIF-8 and ZIF-8 sample. For liposome-coated MOFs, a dialysis bag was used to confine the particles during the release study [35]. The liposome coating material acted as a barrier, potentially slowing down dye release. In

Fig. 2(g), liposome-coated Flu-loaded Fe_3O_4 @ZIF-8 significant released within 6 h, whereas Flu-loaded Fe_3O_4 @ZIF-8 complete released within 2 h. This indicated a slight delay in release due to the liposome barrier. However, under physiological conditions in Fig. 2(h), only around 25% of Flu was released from liposome-coated Flu-loaded MOFs (ZIF-8 and Fe_3O_4 @ZIF-8). These results suggested the effectiveness of liposome as a reservoir in both pH conditions. The release profile of all the samples was analyzed using kinetic models to understand the underlying release mechanisms. The model with R^2 was used and considered the most suitable for explaining the release behavior for each sample, Tables S1 and S2. Burst release observed for 1 and 5 mg/mL of Flu-loaded MOFs in acidic condition could not be accurately described by the models due to the limitation of data. It has been described by degradation of the carrier. In case of pH 7.4, the remaining data points, the Higuchi model provided the highest R^2 values which represented the diffusion of dye from the matrix carrier [27]. This suggested that diffusion could be explain as the dominant release mechanism. Note that, the initial burst release likely reflected the rapid release of loosely bound dye molecules on the MOF surface. Previous work mentioned the potential of ZIF-8 as a pH-sensitive carrier for benzimidazole. In vitro studies under varying pH conditions revealed a controlled and pH-responsive drug release. The Korsmeyer-Peppas model best fitted the release data, suggesting a release mechanism involving a combination of matrix diffusion and erosion from the ZIF-8 structure [36]. Moreover, curcumin (CUR) was used as a model drug to load mSiO_2 @ZIF-8 nanoparticles with 21.39%EE. The system exhibited sensitivity to low pH and demonstrated CUR release kinetics that best fit the Higuchi model [37]. Based on our findings and literature, ZIF-8 carriers provided diffusion-based release and respond to low pH. To control release and potentially reduce burst release, liposome coating could be explored in future work.

3.5. Cytotoxicity study

Cytotoxicity in this study was evaluated using MTT and LDH assays against L929 cells. Morphology of healthy cells were captured and shown in Figs. 3 (a)(b). In contrast, injuries to cells treated with those particles at 100 $\mu\text{g}/\text{mL}$ are shown in Figs. 3 (c)(d). Figs. 3 (e)(h) show the viability bar graph of dyes-loaded MOFs (ZIF-8 and Fe_3O_4 @ZIF-8) without liposome coating, both formulations were around 30 $\mu\text{g}/\text{mL}$ [17,18]. Liposome are expected to reduce the toxicity of MOFs and could increase the number of IC_{50} level. An overall change in cell morphology was confirmed as no toxic of L929 after treated with either 250 $\mu\text{g}/\text{mL}$ of bare liposome or 100 $\mu\text{g}/\text{mL}$ of liposome-coated MOFs, Figs. 4 (a)(c). At higher concentration (500 $\mu\text{g}/\text{mL}$ of liposome-coated MOFs), changing in cell morphology were observed in Figs. 4 (d)(e). The cytotoxicity study confirmed that bare liposome was not toxic to cells (Figs. 4 (f)(g)), with an IC_{50} level exceeding 250 $\mu\text{g}/\text{mL}$. Coating the dye-loaded MOFs with liposome significantly increased the viability value (Figs. 4 (h)(k)) compared to the uncoated materials (Figs. 3 (e)(h)). Herein, the IC_{50} of liposome-coated ZIF-8 and Fe_3O_4 @ZIF-8 increased to 118.21 ± 17.86 $\mu\text{g}/\text{mL}$ and 127.12 ± 9.72 $\mu\text{g}/\text{mL}$, respectively. In the same way, the LDH release was also shown similarly in the opposed side by compared with the cell viability. LDH is a marker for cellular damage or death. When cells are damaged or die, LDH is released into the surrounding medium, making it useful for assessing cell membrane integrity and cytotoxicity in assays, such as cytotoxicity and cellular damage assays.

3.6. Cell uptake

Liposome-coated MOFs were chosen for address cellular uptake due to an increasing of potentially facilitate with cell membrane. At different incubation time (3, 6, and 24 h), both Flu and NiR displayed strong signal within the cells, suggesting successful cellular uptake, Fig. 5. The results showed that liposome platform was able to enhance each MOFs into the cell with less toxicity effect without any permeabilization [38]. These results showed that this liposome platform was one of the best

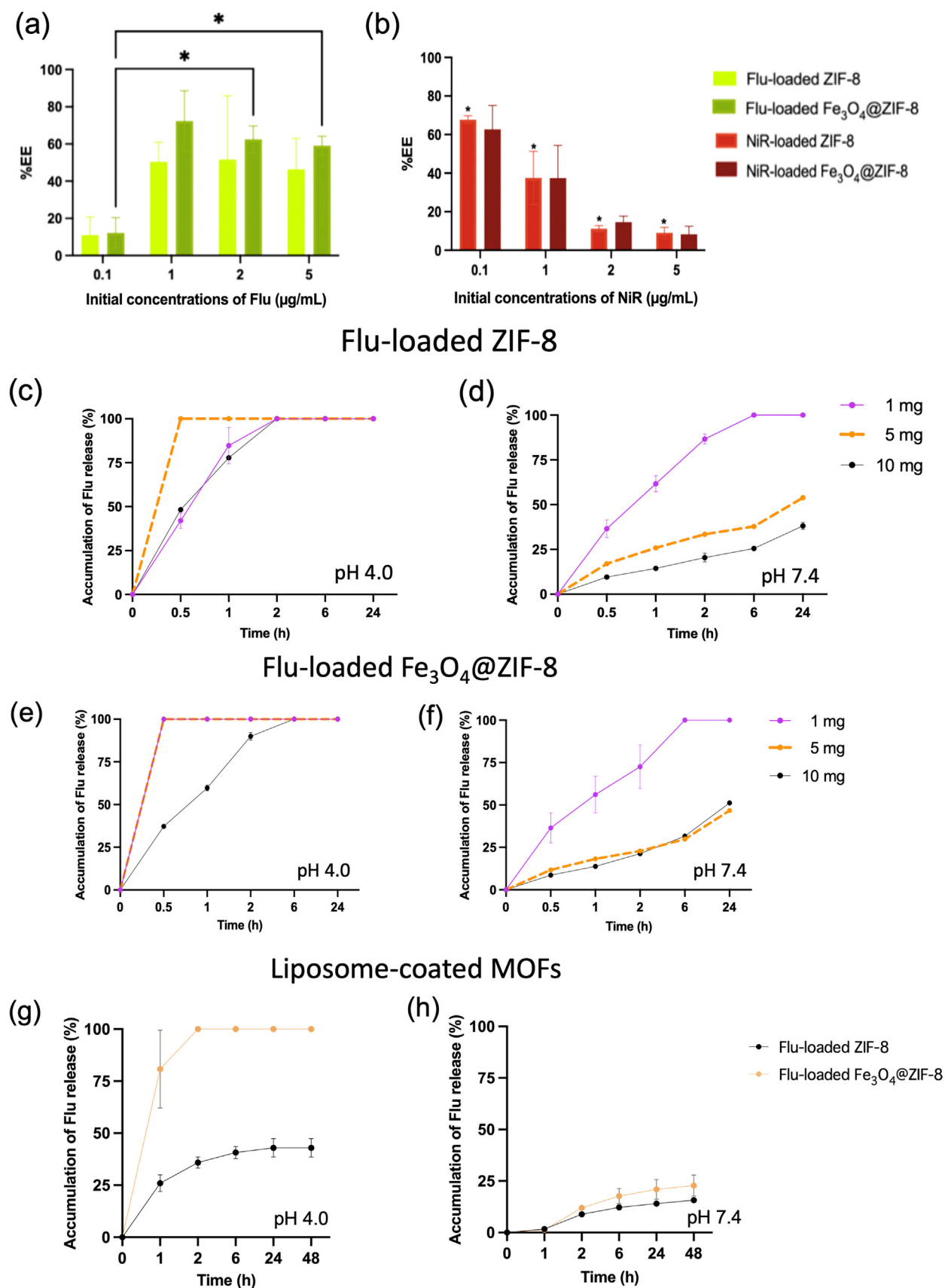


Fig. 2. The encapsulation efficiency (%EE, $n = 3$) of (a) Flu-loaded MOFs (b) NiR-loaded MOFs. The in vitro release study of Flu-loaded ZIF-8 in PBS (c) pH 4 (d) pH 7.4. The in vitro release study ($n = 3$) of Flu-loaded $\text{Fe}_3\text{O}_4@ZIF-8$ in PBS (e) pH 4 and (f) pH 7.4. The In vitro release study of liposome-coated MOFs in PBS (g) pH 4 and (h) pH 7.4.

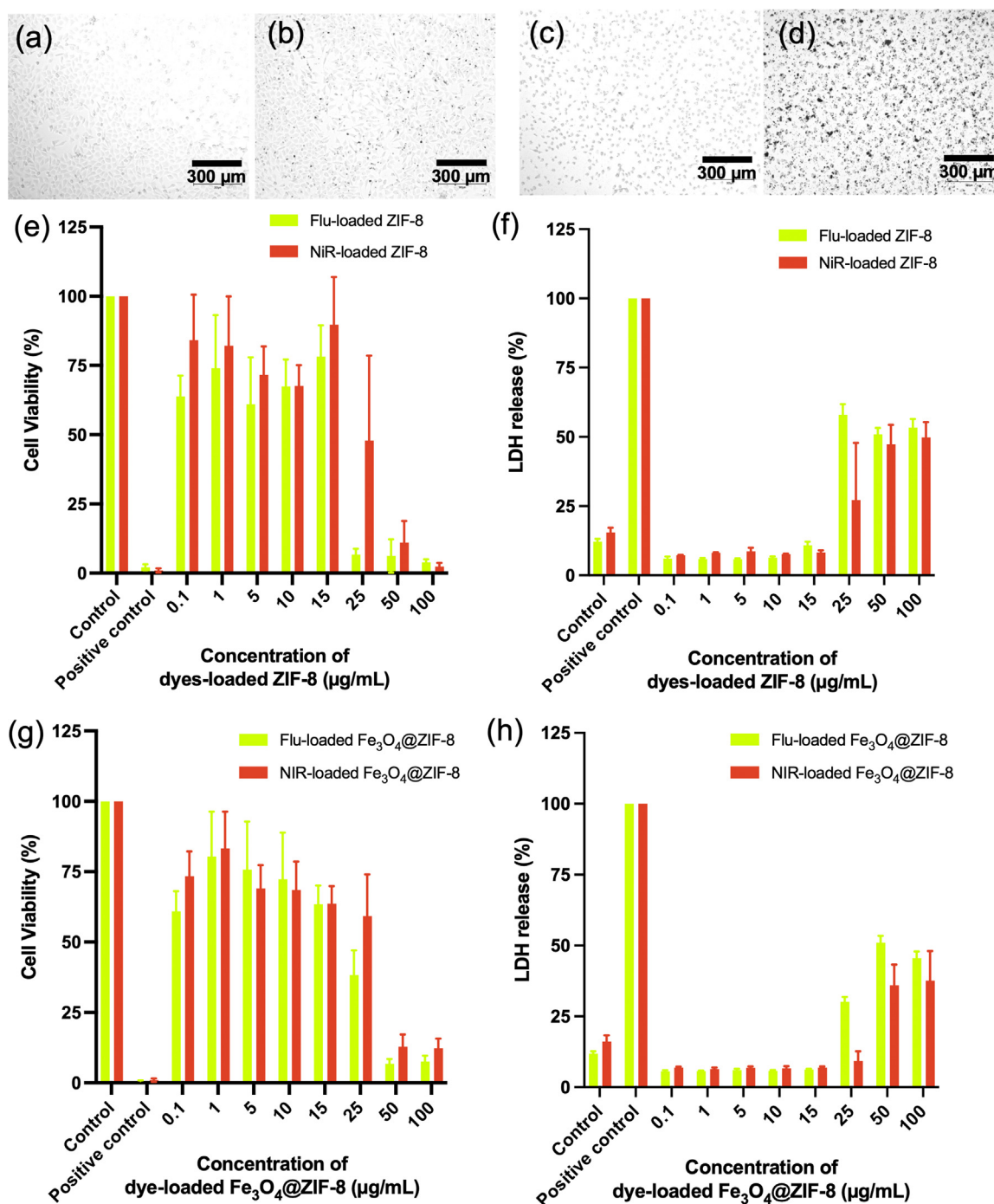


Fig. 3. The morphology of the healthy L929 cell line when was treated with (a) Flu-loaded ZIF-8 (15 µg/mL) and (b) Flu-loaded Fe_3O_4 @ZIF-8 (15 µg/mL). Comparing with the morphology of the injury L929 cell line when was treated with (c) Flu-loaded ZIF-8 and (d) Flu-loaded Fe_3O_4 @ZIF-8 at 100 µg/mL. The cytotoxicity study ($n = 3$) of (e) MTT on dyes-loaded ZIF-8, (f) LDH on dyes-loaded ZIF-8, (g) MTT on dyes-loaded Fe_3O_4 @ZIF-8, and (h) LDH on dyes-loaded Fe_3O_4 @ZIF-8.

candidate to use in the future work which enhance the stability of drug and reduce the toxicity effect of particles inside. Discover a new standard in pharmaceutical innovation with our liposome-coated MOFs, promising enhanced efficacy and precision in drug delivery. This work is hoped to go forward into the animal study and clinical study with the real drug.

This study employed model compounds, Flu and NiR, to investigate the encapsulation of hydrophilic and hydrophobic molecules, respectively, within the ZIF-8 frameworks. While these studies provided insights into the fundamental loading mechanisms, future work is necessary to validate these findings with clinically relevant drugs such as doxorubicin or curcumin. The successful encapsulation of these model com-

pounds showed that post-synthesis loading was a viable option. However, it did not demonstrate the in-situ or one-pot preparation of drug-loaded ZIF-8. Furthermore, while the liposome coating demonstrated its efficacy in mitigating burst release and enhancing biocompatibility on L929 cells, as a recommendation from ISO10993 part 5. The promising preliminary results suggested that this liposomal coating strategy can also be applied to improve the cellular uptake of other nanomaterials. Lastly, the inclusion of Fe_3O_4 nanoparticles in the formulation may provide an opportunity for future diagnostic applications like MRI or CT.

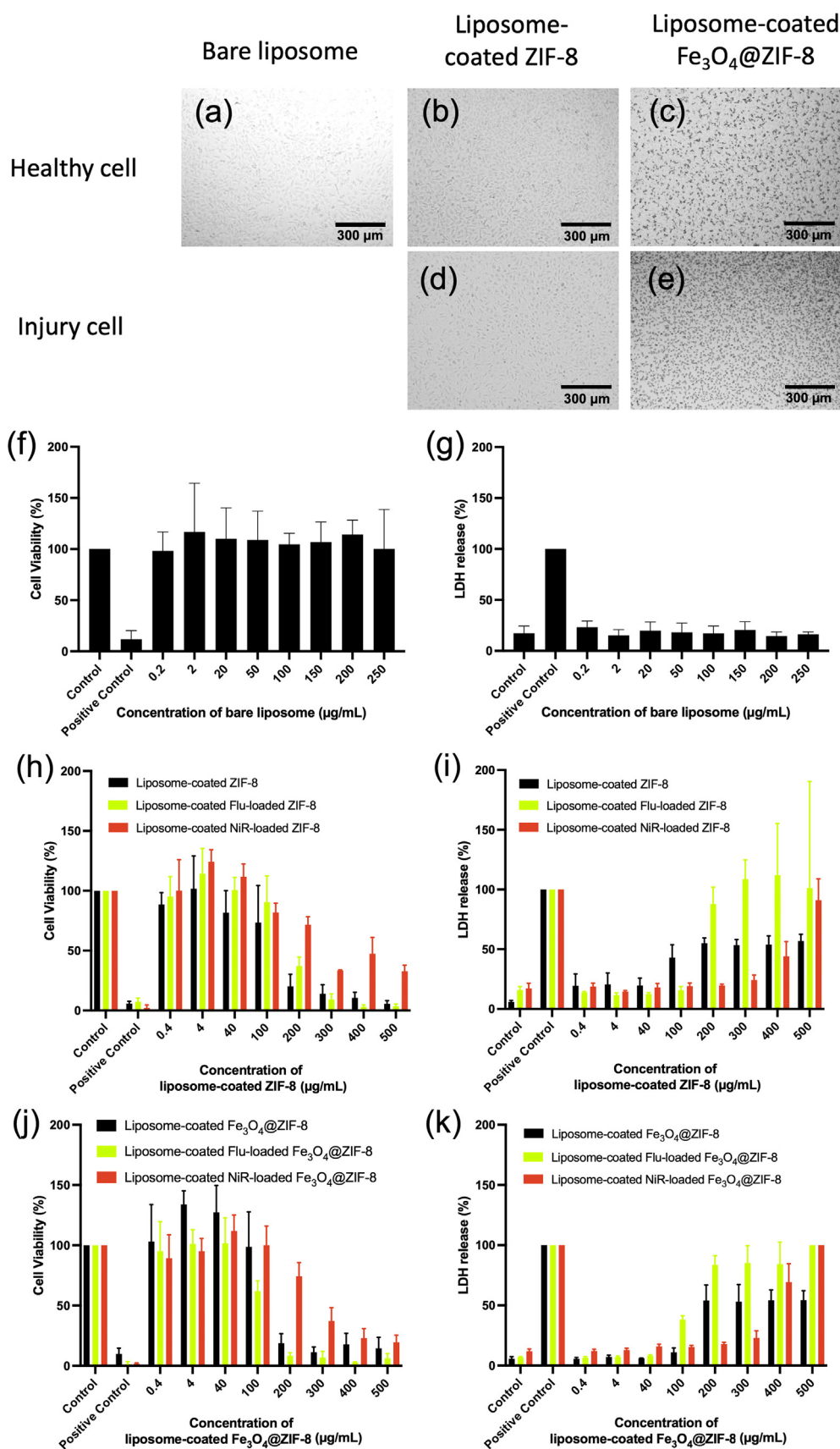


Fig. 4. The morphology of the healthy L929 cell line when was treated with (a) bare liposome (250 µg/mL), (b) liposome-coated ZIF-8 (100 µg/mL) and (c) liposome-coated Fe₃O₄@ZIF-8 (100 µg/mL). Comparing with the morphology of the injury L929 cell line when was treated with (d) liposome-coated ZIF-8 (500 µg/mL) and (e) liposome-coated Fe₃O₄@ZIF-8 (500 µg/mL). In the magnification 10x, the scale bar = 300 µm. The cytotoxicity study (n = 3) of bare liposome with (f) MTT assays and (g) LDH assays. The cytotoxicity study of liposome-coated ZIF-8 with (h) MTT assays and (i) LDH assays. The cytotoxicity study of liposome-coated Fe₃O₄@ZIF-8 with (j) MTT assays and (k) LDH assays.

Cell Uptake

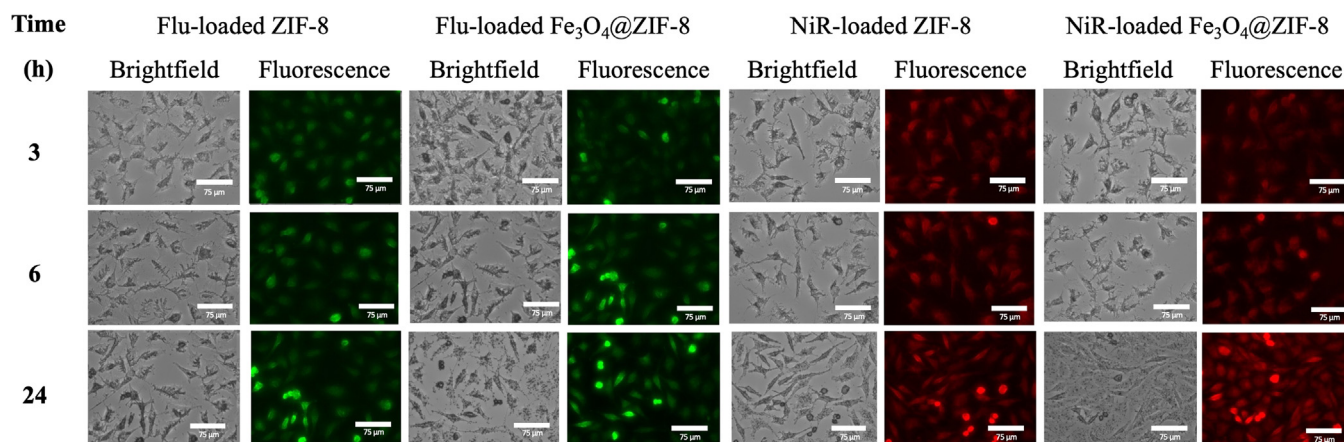


Fig. 5. The cellular uptake of liposome-coated Flu and NiR (50 µg/mL)- loaded MOFs into L929 cells was examined at 3, 6, and 24 h. Scale bar = 75 µm.

4. Conclusion

This study successfully encapsulated fluorescent dyes (Flu, and NiR) in ZIF-8 and Fe₃O₄@ZIF-8, achieving an encapsulation efficiency of around 60%. Liposomes which were formulated with an optimal ratio of DPPC and CHOL were then successfully coated on the MOFs using the solvent injection method. Size, PDI, zeta potential and morphology of the MOFs and liposome-coated MOFs were also investigated to confirm their structure and properties. Coating with liposome indicated a reduction in vitro cytotoxicity by MTT assay. The LDH result supported these findings and confirmed the safety level of coated MOFs at <100 µg/mL. Additionally, the liposome-coated MOFs could increase cellular uptake, as evidenced by Flu and NiR accumulation in the cytoplasm after 24 h of incubation. These findings demonstrated the versatility of these platforms for carrying both hydrophilic and hydrophobic compounds, suggesting potential applications in the drug delivery field.

Declaration of Competing Interest

The authors declare that they have no competing financial interests or personal relationships that may have influenced the work reported in this study.

CRediT authorship contribution statement

Natchanon Ratanapun: Writing – original draft, Visualization, Software, Methodology, Investigation, Formal analysis. **Komgrit Eawsakul:** Writing – review & editing, Methodology, Formal analysis. **Naruemon Setthaya:** Writing – review & editing, Methodology, Investigation, Formal analysis. **Chakkresit Chindawong:** Writing – review & editing, Methodology, Investigation, Formal analysis. **Wei Guo Song:** Writing – review & editing. **Chawan Manaspon:** Writing – review & editing, Validation, Supervision, Software, Methodology, Investigation, Conceptualization. **Pagasukon Mekrattanachai:** Writing – review & editing, Validation, Supervision, Software, Methodology, Investigation, Funding acquisition, Conceptualization.

Acknowledgements

The authors are grateful for the fundamental fund from the University of Phayao (FF67-1848/2567). The authors would like to thank the Unit of Excellence on Advanced Nanomaterials which was supported by the Thailand Science Research and Innovation Fund and the University of Phayao. This research work was supported by Chiang Mai University.

Supplementary materials

Supplementary material associated with this article can be found, in the online version, at doi:10.1016/j.chphma.2025.08.004.

References

- [1] S. Bamrungsap, Z. Zhao, T. Chen, L. Wang, C. Li, T. Fu, W. Tan, Nanotechnology in therapeutics: A focus on nanoparticles as a drug delivery system, *Nanomed. (Lond.)* 7 (2012) 1253–1271, doi:10.2217/nnm.12.87.
- [2] L. Sun, H. Liu, Y. Ye, Y. Lei, R. Islam, S. Tan, R. Tong, Y.B. Miao, L. Cai, Smart nanoparticles for cancer therapy, *Sig. Transduct. Target. Ther.* 8 (2023) 418, doi:10.1038/s41392-023-01642-x.
- [3] J. Halder, D. Pradhan, P. Biswasroy, V.K. Rai, B. Kar, G. Ghosh, G. Rath, Trends in iron oxide nanoparticles: A nano-platform for theranostic application in breast cancer, *J. Drug. Target.* 30 (2022) 1055–1075, doi:10.1080/1061186X.2022.2095389.
- [4] H. Park, A. Otte, K. Park, Evolution of drug delivery systems: From 1950 to 2020 and beyond, *J. Control. Release* 342 (2022) 53–65, doi:10.1016/j.jconrel.2021.12.030.
- [5] A.M. Wright, M.T. Kapelewski, S. Marx, O.K. Farha, W. Morris, Transitioning metal-organic frameworks from the laboratory to market through applied research, *Nat. Mater.* 24 (2025) 178–187, doi:10.1038/s41563-024-01947-4.
- [6] C. Li, J. Wang, Y. Wang, H. Gao, G. Wei, Y. Huang, H. Yu, Y. Gan, Y. Wang, L. Mei, Recent progress in drug delivery, *Acta Pharm. Sin. B* 9 (2019) 1145–1162, doi:10.1016/j.apsb.2019.08.003.
- [7] J. Cao, X. Li, H. Tian, Metal-organic framework (MOF)-based drug delivery, *Curr. Med. Chem.* 27 (2020) 5949–5969, doi:10.2174/092986732666190618152518.
- [8] H. Kaur, G.C. Mohanta, V. Gupta, D. Kukkar, S. Tyagi, Synthesis and characterization of ZIF-8 nanoparticles for controlled release of 6-mercaptopurine drug, *J. Drug Deliv. Sci. Technol.* 41 (2017) 106–112, doi:10.1016/j.jddst.2017.07.004.
- [9] J.A. Greathouse, M.D. Allendorf, The interaction of water with MOF-5 simulated by molecular dynamics, *J. Am. Chem. Soc.* 128 (2006) 10678–10679, doi:10.1021/ja063506b.
- [10] F. Demir Duman, A. Monaco, R. Foulkes, C.R. Becer, R.S. Forgan, Glycopolymer-functionalized MOF-808 nanoparticles as a cancer-targeted dual drug delivery system for carboplatin and floxuridine, *ACS Appl. Nano Mater.* 5 (2022) 13862–13873, doi:10.1021/acsnano.2c01632.
- [11] Y. Dai, Q. Tang, Z. Zhang, C. Yu, H. Li, L. Xu, S. Zhang, Z. Zou, Enhanced mechanical, thermal, and UV-shielding properties of poly (vinyl alcohol)/metal-organic framework nanocomposites, *RSC Adv.* 8 (2018) 38681–38688, doi:10.1039/C8RA07143H.
- [12] A. Ma, R. Zhang, Facile synthesis of redox-responsive paclitaxel drug release platform using metal-organic frameworks (ZIF-8) for gastric cancer treatment, *Mater. Res. Express* 7 (2020) 095402, doi:10.1088/2053-1591/abb2ce.
- [13] Y. Wang, M. Zeng, T. Fan, M. Jia, R. Yin, J. Xue, L. Xian, P. Fan, M. Zhan, Biomimetic ZIF-8 nanoparticles: A novel approach for biomimetic drug delivery systems, *Int. J. Nanomed.* 19 (2024) 5523–5544, doi:10.2147/IJN.S462480.
- [14] X. Sun, F. Li, L. Yuan, Z. Bing, X. Li, K. Yang, pH-responsive resveratrol-loaded ZIF-8 nanoparticles modified with tannic acid for promoting colon cancer cell apoptosis, *J. Biomed. Mater. Res. B* 112 (2024) e35320, doi:10.1002/jbm.b.35320.
- [15] M. Alizadeh, P.A. Azar, S.A. Mozaffari, H. Karimi-Maleh, A.M. Tamaddon, A DNA based biosensor amplified with ZIF-8/ionic liquid composite for determination of mitoxantrone anticancer drug: An experimental/docking investigation, *Front. Chem.* 8 (2020) 814, doi:10.3389/fchem.2020.00814.
- [16] P. Chen, M. He, B. Chen, B. Hu, Size- and dose-dependent cytotoxicity of ZIF-8 based on single cell analysis, *Ecotoxicol. Environ. Saf.* 205 (2020) 111110, doi:10.1016/j.ecoenv.2020.111110.
- [17] P. Mekrattanachai, N. Sethaya, C. Chindawong, B. Yotnoi, W.G. Song, C. Manaspon, Synthesis of hydrogels incorporating core-shell structured Fe₃O₄@ZIF-8 as

- bio-nanocomposite carriers for drug delivery, *Aust. J. Chem.* 76 (2023) 201–208, doi:10.1071/CH22224.
- [18] P. Mekrattanchai, N. Sethaya, C. Chindawong, B. Yotnoi, W.G. Song, N. Ratanapun, S. Tambunlertchai, C. Manaspon, Zeolitic imidazolate framework-8-loaded hydrogels as a highly biocompatible carrier for drug delivery applications, *J. Biomim. Biomater. Biomed. Eng.* 60 (2023) 29–42, doi:10.4028/p-268hc7.
- [19] R.S. Chouhan, M. Horvat, J. Ahmed, N. Alhokbany, S.M. Alshehri, S. Gandhi, Magnetic nanoparticles—A multifunctional potential agent for diagnosis and therapy, *Cancers* 13 (2021) 2213, doi:10.3390/cancers13092213.
- [20] R. Ghazi, T.K. Ibrahim, J.A. Nasir, S. Gai, G. Ali, I. Boukhris, Z. Rehman, Iron oxide based magnetic nanoparticles for hyperthermia, MRI and drug delivery applications: A review, *RSC Adv.* 15 (2025) 11587–11616, doi:10.1039/D5RA00728C.
- [21] Y. Wu, Q. Huang, J. Wang, Y. Dai, M. Xiao, Y. Li, H. Zhang, W. Xiao, The feasibility of targeted magnetic iron oxide nanoagent for noninvasive IgA nephropathy diagnosis, *Front. Bioeng. Biotechnol.* 9 (2021) 755692, doi:10.3389/fbioe.2021.755692.
- [22] J. Nowak-Jary, B. Machnicka, Comprehensive analysis of the potential toxicity of magnetic iron oxide nanoparticles for medical applications: Cellular mechanisms and systemic effects, *Int. J. Mol. Sci.* 25 (2024) 12013, doi:10.3390/ijms252212013.
- [23] A. Samad, Y. Sultana, M. Aqil, Liposomal drug delivery systems: An update review, *Curr. Drug. Deliv.* 4 (2007) 297–305, doi:10.2174/156720107782151269.
- [24] E. Zingale, A. Romeo, S. Rizzo, C. Cimino, A. Bonaccorso, C. Carbone, T. Musumeci, R. Pignatello, Fluorescent nanosystems for drug tracking and theranostics: Recent applications in the ocular field, *Pharmaceutics* 14 (2022) 955, doi:10.3390/pharmaceutics14050955.
- [25] E. Jaradat, E. Weaver, A. Meziane, D.A. Lamprou, Microfluidic paclitaxel-loaded lipid nanoparticle formulations for chemotherapy, *Int. J. Pharm.* 628 (2022) 122320, doi:10.1016/j.ijpharm.2022.122320.
- [26] M. Askarizadeh, N. Esfandiari, B. Honarvar, S.A. Sajadian, A. Azdarpour, Kinetic modeling to explain the release of medicine from drug delivery systems, *ChemBio-Eng Rev.* 10 (2023) 1006–1049, doi:10.1002/cben.202300027.
- [27] W.M. Saltzman, *Drug delivery: Engineering principles For Drug Therapy*, Oxford University Press, New York, 2001.
- [28] D. Guimarães, A. Cavaco-Paulo, E. Nogueira, Design of liposomes as drug delivery system for therapeutic applications, *Int. J. Pharm.* 601 (2021) 120571, doi:10.1016/j.ijpharm.2021.120571.
- [29] H. Nsairat, A.A. Ibrahim, A.M. Jaber, S. Abdelghany, R. Atwan, N. Shalan, H. Abdelnabi, F. Odeh, M. El-Tanani, W. Alshaer, Liposome bilayer stability: Emphasis on cholesterol and its alternatives, *J. Liposom. Res.* 34 (2024) 178–202, doi:10.1080/08982104.2023.2226216.
- [30] J. Huang, X. Mo, H. Fu, Y. Sun, Q. Gao, X. Chen, J. Zou, Y. Yuan, J. Nie, Y. Zhang, Tyndall-effect-enhanced supersensitive naked-eye determination of mercury (II) ions with silver nanoparticles, *Sens. Actuators B-Chem.* 344 (2021) 130218, doi:10.1016/j.snb.2021.130218.
- [31] N.V.N. Jyothi, P.M. Prasanna, S.N. Sakarkar, K.S. Prabha, P.S. Ramaiah, G. Srawan, Microencapsulation techniques, factors influencing encapsulation efficiency, *J. Microencapsul.* 27 (2010) 187–197, doi:10.3109/02652040903131301.
- [32] C. Adhikari, A. Das, A. Chakraborty, Zeolitic imidazole framework (ZIF) nanospheres for easy encapsulation and controlled release of an anticancer drug doxorubicin under different external stimuli: A way toward smart drug delivery system, *Mol. Pharm.* 12 (2015) 3158–3166, doi:10.1021/acs.molpharmaceut.5b00043.
- [33] N.A. Soomro, Q. Wu, S.A. Amur, H. Liang, A.U. Rahman, Q. Yuan, Y. Wei, Natural drug physcion encapsulated zeolitic imidazolate framework, and their application as antimicrobial agent, *Colloid. Surf. B Biointerfaces* 182 (2019) 110364, doi:10.1016/j.colsurfb.2019.110364.
- [34] S. Mohammadkhal, M. Ramezanzadeh, H.E. Mohammadloo, B. Ramezanzadeh, R. Ghamsarizade, Construction of a nano-micro nacre-inspired 2D-MoS₂-MOF-glutamate carrier toward designing a high-performance smart epoxy composite, *J. Ind. Eng. Chem.* 121 (2023) 358–377, doi:10.1016/j.jiec.2023.01.039.
- [35] L.R. de Moura Ferraz, A.É.G.A. Tabosa, D.D.S. da Silva Nascimento, A.S. Ferreira, V. de Albuquerque Wanderley Sales, J.Y.R. Silva, S.A. Júnior, L.A. Rolim, J.J. de Souza Pereira, P.J. Rolim-Neto, ZIF-8 as a promising drug delivery system for benzimidazole: Development, characterization, in vitro dialysis release and cytotoxicity, *Sci. Rep.* 10 (2020) 16815, doi:10.1038/s41598-020-73848-w.
- [36] L.R. de Moura Ferraz, A.É.G.A. Tabosa, D.D.S. da Silva Nascimento, A.S. Ferreira, J.Y.R. Silva, S.A. Junior, L.A. Rolim, P.J. Rolim-Neto, Benzimidazole in vitro dissolution release from a pH-sensitive drug delivery system using Zif-8 as a carrier, *J. Mater. Sci.: Mater. Med.* 32 (2021) 59, doi:10.1007/s10856-021-06530-w.
- [37] M. Chen, F. Song, N. Wu, H. Luo, X. Cai, Y. Li, Corn-like mSiO₂@ ZIF-8 composite load with curcumin for target cancer drug-delivery system, *ChemistrySelect* 7 (2022) e202204213, doi:10.1002/slct.202204213.
- [38] M.U. Amin, S. Ali, M.Y. Ali, I. Tariq, U. Nasrullah, S.R. Pinnapreddy, C. Wölk, U. Bakowsky, J. Brüsler, Enhanced efficacy and drug delivery with lipid coated mesoporous silica nanoparticles in cancer therapy, *Eur. J. Pharm. Biopharm.* 165 (2021) 31–40, doi:10.1016/j.ejpb.2021.04.020.